Available online at www.sciencedirect.com

ScienceDirect

Materials Today: Proceedings XX (2016) XXX–XXX

materialstoday: PROCEEDINGS

www.materialstoday.com/proceedings

ANM2016

Synthesis and characterization of efficient TiO_2 mesoporous photocatalysts

Evgeni Ovodok[a], Hanna Maltanava[a]*, Sergey Poznyak[a], Maria Ivanovskaya[a], Alexander Kudlash[b], Nico Scharnagl[c], Joao Tedim[d]

[a]*Research Institute for Physical Chemical Problems, Belarusian State University, Leningradskaya str. 14, 220030 Minsk, Belarus*
[b]*Chemistry Department, Belarusian State University, Nezavisimosti ave 4, 220030 Minsk, Belarus*
[c]*Helmholtz-Zentrum Geesthacht Centre for Materials and Coastal Research GmbH, Max-Planck-Straße 1, 21502 Geesthacht, Germany*
[d]*Department of Materials and Ceramics Engineering, CICECO-Aveiro Institute of Materials, University of Aveiro, Campus Universitário de Santiago, 3810-193 Aveiro, Portugal*

Abstract

Mesoporous TiO_2 powder with large surface area and high porosity was prepared *via* template-free method of heat-stimulated oxidizing destruction of TiC by HNO_3. Anatase crystalline phase of as-prepared and annealed at 200−400 °C titania was confirmed by XRD technique. Surface nitrate-nitro groups responsible for high adsorption capacity of the TiO_2 powders were studied by FTIR spectroscopy. The annealing temperature can be used as a factor for regulation of titania morphology and structural properties. The rise in the annealing temperature higher than the temperature of nitrate-nitro groups decomposition induces the growth of TiO_2 crystallites, decreasing porosity and surface area, the drop of adsorption capacity, and improving photocatalytic activity under UV irradiation.

Selection and Peer-review under responsibility of 7th International Conference on Advanced Nanomaterials.

Keywords: Titanium dioxide; Mesoporous materials; Photocatalyst

* Corresponding author. Tel.: +375-17-209-53-02.
E-mail address: annamaltanova@gmail.com

Selection and Peer-review under responsibility of 7th International Conference on Advanced Nanomaterials.

1. Introduction

Among various oxide semiconductors, titania is considered as the most important photocatalyst due to its biological and chemical inertness, strong oxidizing power, nontoxicity, and long-term stability against photo- and chemical corrosion [1−4]. Titania with large surface area and high porosity is often required to achieve high efficiency associated with photocatalytic applications [5]. Recently, ordered mesoporous TiO_2 films and powders attracted considerable interest as potential photocatalysts owing to their large surface area and narrow pore size distribution, while retaining a crystalline framework [1−10]. Moreover, the mesoporous network promotes the diffusion of reactants and products, as well as facilitates the access to reactive sites on the surface of the photocatalysts [11, 12]. Firstly, mesoporous TiO_2 was synthesized using alkyl phosphate as a structure-directing template and titanium isopropoxide *bis*-acetylacetonate as a Ti-containing precursor [13]. Since then, many efforts have been made to synthesize mesoporous TiO_2 films and powders with various mesostructures, pore-wall parameters, morphology, doping and crystallization degree [14−19]. The development of ordered large-pore-size mesoporous TiO_2 material has been mostly related with the use of surfactants or block polymers as templates. The template removal by calcination generates high-surface-area mesoporous TiO_2. However, thermal treatment at high temperatures may have undesirable effects such as the collapse of mesoporous framework and loss of surface area due to facile crystallization of TiO_2 and subsequent crystal growth [20].

The synthesis of mesoporous TiO_2 through template-free methods is an important issue from industrial and environmental points of view. Most of the template-free routes for the synthesis of mesoporous TiO_2 materials are related with the hydrolysis or oxidation reactions using nitric acid and phosphoric acid as a catalytic or oxidizing agent [21−23]. Nevertheless, the influence of inorganic acids on the process and the material structures has not been investigated systematically. This paper presents a detailed study of the fabrication of mesoporous TiO_2 using a mild, one-step HNO_3 oxidation of TiC at 70 °C, firstly reported in [23] with some modifications. In our work we used a comparatively lower concentration of HNO_3 to save some non-oxidized carbon species in the obtained TiO_2 powder. Attention was given to the characterization of structure, surface properties and photocatalytic activity of the obtained material.

2. Experimental

2.1. TiO_2 synthesis

1.5 g of TiC (in black powder form) was placed into a three-neck round bottom flask equipped with a stir bar, a dropping funnel filled with 18 mL of 4 M HNO_3 and a reflux condenser. The nitric acid was added dropwise into the flask with TiC with a rate of 2 drops per second. The synthesis was carried out on a water bath at 70 °C. After complete addition of nitric acid the reaction was allowed to run for 1 h. After that reaction time, a yellow precipitate was formed at the bottom of the flask. The precipitate was separated by filtration and washed 3 times with ethanol. Afterwards, the resulting powder was dried at 70 °C in air and then annealed at different temperatures (the heating rate was 10 °C/min^{-1}).

2.2. Characterization

The TiO_2 crystal structure was examined by X-ray diffraction on a PANalytical X'Pert PRO MRD (Multi-Purpose Research Diffractometer, Holland) with modular construction using CuKα-radiation. Recording speed was 0.4 °/min.

The surface area and porosity of the samples were measured on a Micromeritics ASAP 2020 system using nitrogen at 77 K.

The particle size and morphology were characterized by scanning electron microscopy (SEM) using a TESCAN Vega3 SB microscope operating at 20.1 kV. Samples for SEM were prepared by scattering of dispersed powder onto holder coated with solution of liquid carbon "PlanoCarbon" and the solvent was evaporated immediately under ambient conditions. No sputtering was used for prevent samples charching by electron beam.

The thermal analysis of the TiO_2 powders was carried out on a NETZSCH STA 449C instrument using an alumina crucible over the temperature range from 30 to 800 °C in air. The heating rate was 10^o per min.

Fourier transform infrared (FTIR) spectra were collected on an AVATAR-330 (Thermo Nicolet) spectrometer supplied with a diffuse reflectance accessory in the wavenumber range from 400 to 4000 cm^{-1}.

Adsorption of Rhodamine on the powder was performed in 2 mL Eppendorf tubes. 10 mg of TiO_2 powder was dispersed in 1.5 mL of 5 mM Rhodamine B (RhB) solution. The tubes were shaken during 1 h in dark at room temperature. Then, the powder was separated by centrifugation and solution was analysed by an UV–vis spectrophotometer (Shimadzu UV- 2550).

2.3. Measurement of photocatalytic activity

Photocatalytic activities of the TiO_2 samples were evaluated by the degradation of RhB aqueous solutions under UV irradiation. In each experiment, 80 mg of metal oxide catalyst was dispersed in 80mL of 0.02 mM RhB solution in a quartz cell at 20 °C and the dispersion was irradiated during various times. The system was mildly stirred using a magnetic stirrer. A mercury lamp (NARVA UVK-125-2) was used as the UV light source; the concentration of RhB was analyzed by an UV–vis spectrophotometer.

3. Results and discussion

3.1. X-ray diffraction

Oxidation of black TiC powder by concentrated nitric acid gives a yellowish powder with fine-dispersed structure. X-ray diffraction patterns of the resultant material dried at 70 °C and than annealed at different temperatures are shown in Fig. 1. Only broadened peaks characteristic of anatase TiO_2 phase can be seen in the diffractograms, indicating that titanium carbide is completely oxidized by nitric acid resulting in the formation of fine-grained titanium dioxide [24]. The mean size of the TiO_2 anatase crystallites was estimated by the width of the (101) peak using Debye–Scherrer equation ($D = 0.9\lambda/k\cos\theta$, where k is the full width at half-maximum (FWHM) of the peak, θ is the angle of diffraction, and λ is the wavelength of the X-ray radiation) and is about 4 nm for dried sample and 3.9 nm and 7.4 nm for the samples annealed at 200 and 400 ^{o}C, respectively.

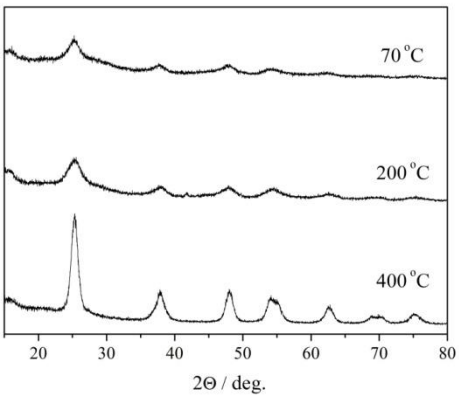

Fig. 1. X-ray diffractograms of TiO_2 powders obtained from TiC and annealed at different temperatures.

3.2. Scanning electron microscopy

SEM images clearly show that large well-faceted crystals of TiC were transformed to fine-porous micron-sized aggregates of titanium dioxide nanocrystallites after treatment with HNO_3 (Fig. 2).

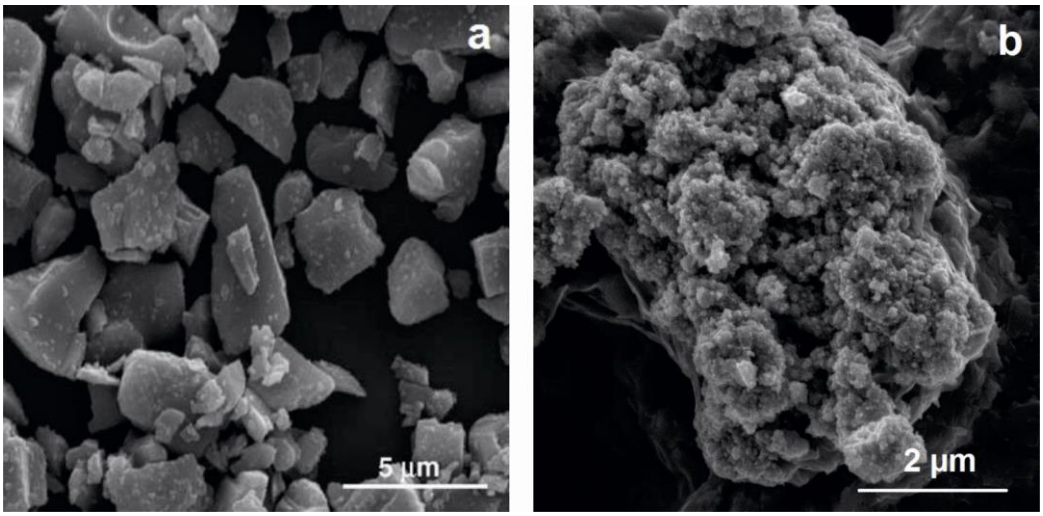

Fig. 2. Scanning electron micrographs of (a) TiC precursor, and (b) TiO_2 powder annealed at 200 °C.

3.3. Brunauer-Emmett-Teller (BET) analysis

The mesoporous structure of the powder prepared by oxidative destruction of titanium carbide was investigated by N_2 adsorption-desorption isotherm measurements. The isotherms of both as-prepared dried powder and the powder annealed at 200 °C can be classified as type IV according to the IUPAC recommendations [25], which is indicative of mesoporous materials. The structural properties of the TiO_2 powders dried at 70 °C and annealed at different temperatures are summarized in Table 1. The powder annealed at 200 °C has quite large BET surface area and total pore volume reaching values of 353 m^2 g^{-1} and 0.300 cm^3 g^{-1}, respectively. However, the surface area and pore volume of the TiO_2 powders decrease appreciably after annealing at 400 °C that indicates beginning of the mesoporous structure collapse.

Table 1. Structural characteristics and adsorption capacity (RhB) of the TiO_2 powders synthesized from the reaction between TiC and HNO_3 and then annealed at different temperatures in air.

Annealing temperature (°C)	BET surface area (m^2 g^{-1})	Average pore diameter (nm)	Total pore volume (cm^3 g^{-1})	Adsorption capacity of RhB (mg g^{-1})*
70	290	3.1	0.224	40
200	353	3.4	0.300	35
400	135	5.5	0.185	0.5

*Adsorption of RhB from 5mM solution

3.4. FTIR spectroscopy

Structural characteristics of the TiO_2 samples were also estimated by FTIR spectroscopy. Infrared spectra of the TiO_2 powders prepared from titanium carbide and annealed at different temperatures are shown in Fig. 3.

The dominating wide band at 400÷850 cm^{-1} is attributed to vibrations in octahedrons [TiO_6]. It is a superposition of several normal ν(Ti−O) vibrations characteristic of titanium dioxide. There are also two intensive bands related to

deformation δ(HO−H) vibrations at 1629 cm^{-1} and asymmetric ν_{as}(O−H) vibrations at 3200÷3400 cm^{-1} of water molecules. The region from 800 to 1800 cm^{-1} shows vibrations of nitro, nitrates and carboxylate groups (Fig. 3b).

Nitrate anion can be coordinated to the surface contacting the Ti as a monodentate, symmetric or asymmetric chelate bidentate, and bidentate bridging group. The symmetry of such ions differs slightly (C_{2v} or C_s), therefore it is difficult to distinguish them in the IR spectra. A bound nitrate group gives three normal vibrations (ν_5 = 1515÷1565 cm^{-1}, ν_1 = 1250÷1295 cm^{-1} and ν_2 = 1015÷1050 cm^{-1}), depending on the coordination of the nitrate group [26] and composite ($\nu_1+\nu_4$) vibration, which is split according to the type of nitrate group coordination in the 1645÷1710 cm^{-1} range [27]. For the as-prepared TiO_2 sample, composite ($\nu_1+\nu_4$) vibration is observed from unbound nitrate group (at 1684 cm^{-1}) and from bidentate one (at 1629 and 1711 cm^{-1}). For the TiO_2 sample annealed at 200°C in this region there are vibrations from unbound nitrate group (at 1680 cm^{-1}), monodentate group (at 1665 and 1680 cm^{-1}) and bidentate one (at 1644 and 1710 cm^{-1}). The lines at 1407 and 1107 cm^{-1} are the symmetric and asymmetric stretching vibrations of nitro group, respectively. All bands belonging to the nitrate and nitro groups are reduced upon annealing the samples, and after heat treatment at 400 °C the vibrations related to nitrate and nitro groups are not observed.

The broad absorption band at 2000 cm^{-1} may be due to the appearance of complexes with CO adsorbed on the TiO_2 surface.

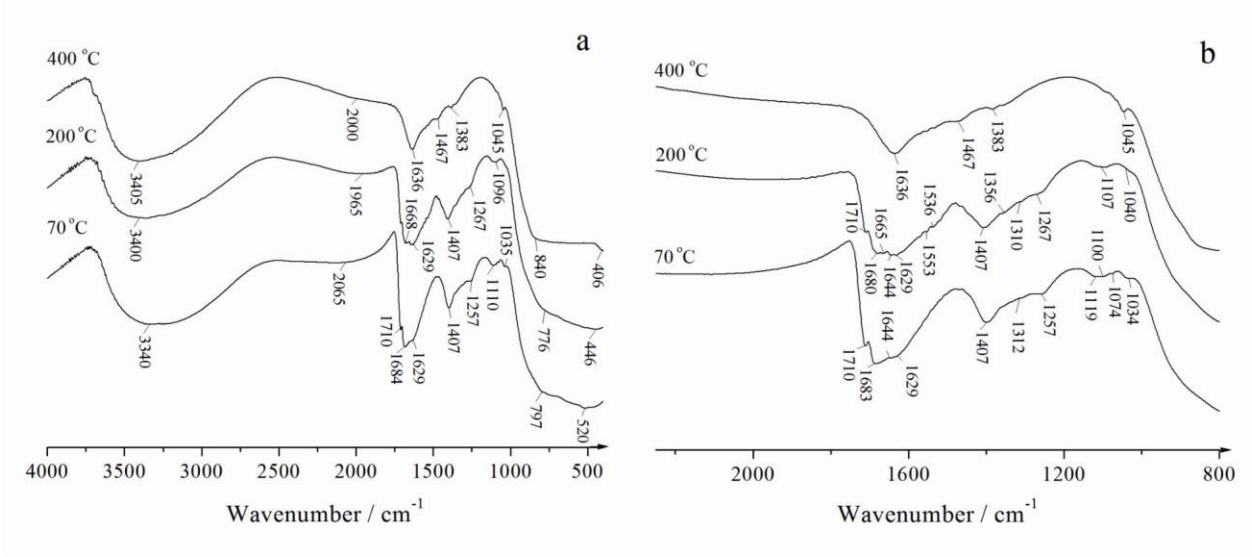

Fig. 3. Full (a) and magnificated part (b) of FTIR spectra recorded for the TiO_2 powders annealed at 70 °C, 200 °C, and 400 °C.

3.5. Thermal analysis

According to the thermal analysis data the weight loss of the as-prepared powder occurs in three steps (Fig. 4.):

1) Up to 160 °C a weight loss of 11 % is observed belonging to removal of weakly bound water and nitric acid physically adsorbed on the surface.

2) From 160 °C to 350 °C the weight loss corresponds to 15 %. It can be associated with the decomposition of nitrate and nitro surface species, burning of carbon residues, removal of oxidized carbon species and chemically bound water. The presence of oxidized carbon species in the as-synthesized material is supported by the fact that after annealing the powder in an inert atmosphere (argon) at 400 °C its color is changed from yellowish to black.

3) Above 350 **°C** the decrease in weight is only 2.2 %. This weight loss accompanied by a slight exothermic effect that could be related to the elimination of tightly bound OH-groups, structural water and the most stable carbon species.

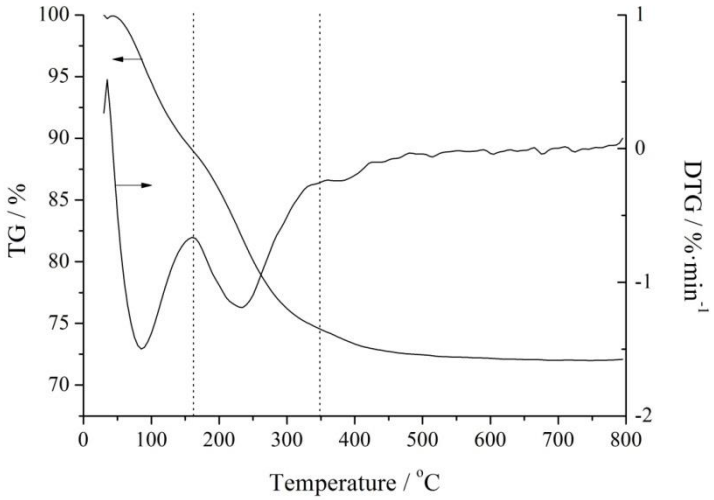

Fig. 4. TG/DTG curves for the TiO_2 powder obtained by oxidation of TiC with nitric acid.

3.6. Rhodamine B adsorption on the TiO_2 powders

The 'dark' adsorption capacity of the samples was estimated using a positively charged dye (RhB) (Table 1). The samples annealed at 70 °C and 200 °C adsorb 40 and 35 mg/g of RhB, respectively. Increasing the annealing temperature leads to a lowering of the adsorption capacity. The sample annealed at 400 °C almost does not adsorb RhB in neutral solution.

3.7. Rhodamine B photodegradation in TiO_2 slurries under UV irradiation

The synthesized TiO_2 samples are photocatalytically active in degradation of Rhodamine B in aqueous solutions, as depicted in Fig. 5.

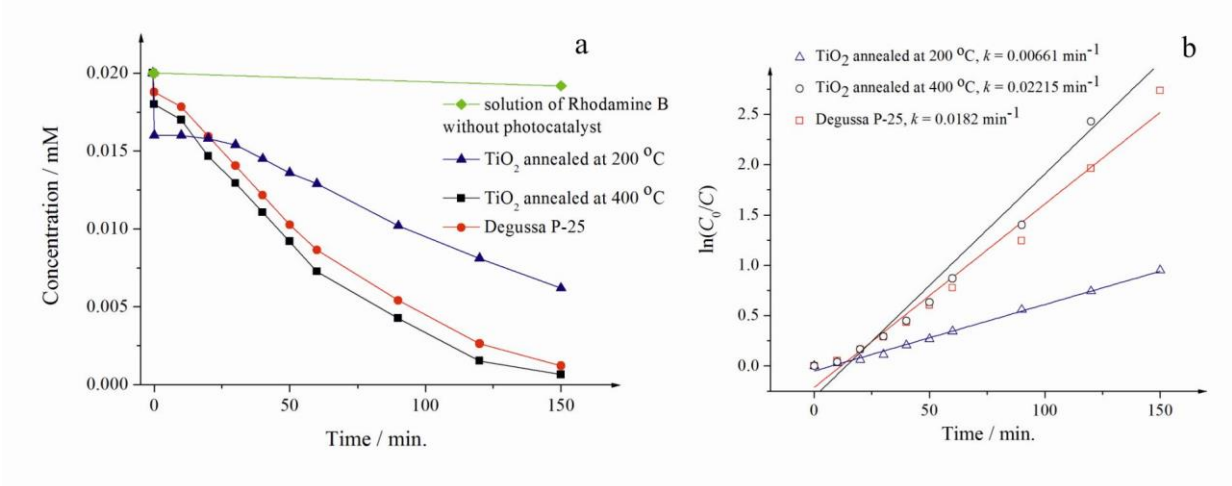

Fig. 5. Photocatalytic activity of the TiO_2 powders annealed at different temperatures for photodegradation of RhB under UV irradiation: a) variation of the RhB concentration as a function of irradiation time and b) fitting of experimental data using first-order kinetic model.

The kinetics of Rhodamine B photodecomposition on the oxide surface can be described by the first-order equation [28]:

$$\ln\left(\frac{C_0}{C}\right) = kt, \qquad (1)$$

where k is the rate constant (min^{-1}), C_0 is the initial concentration of the dye, and C is the actual concentration of the dye at irradiation time t. Fig. 5b presents the linear relationship between $\ln(C_0/C)$ and irradiation time. The rate constant k is determined from the slope of the linear $\ln(C_0/C)$ *vs* t plots. The value of k gives an indication of the photocatalytic activity. The rate constant for the TiO_2 sample annealed at 200 °C is 0.0066 min^{-1}. Increasing the annealing temperature leads to a higher photoactivity of the TiO_2 powder. The photoactivity of the sample annealed at 400 °C is close to that of commercial TiO_2 photocatalyst Degussa P-25 in the UV range. The rate constants for the TiO_2 sample annealed at 400 °C and for Degussa P-25 are 0.02215 min^{-1} and 0.0182 min^{-1}, respectively.

3.8. Discussion about formation mechanism and properties of mesoporous TiO_2

On the basis of the experimental results obtained the mechanism of mesoporous titania formation from TiC powder during oxidation by nitric acid is proposed.

TiC powder does not react at a detectable rate with nitric acid at room temperature. The reaction begins only after thermal activation. Oxidation of titanium carbide with an intensive liberation of gases is observed at 70 °C. In a first step, titanium carbide is oxidized by nitric acid to titanium(IV) nitrate (2). However, titanium(IV) nitrate is unstable in aqueous solutions and rapidly hydrolyzes to titanium(IV) oxynitrate (3). Then, titanium(IV) oxynitrate can undergo stepwise hydrolysis up to hydrated forms of titania $TiO_2 \cdot xH_2O$ (4) or can directly oxidize titanium carbide (5). The overall process of the TiO_2 formation can be illustrated by the equation (6).

$$TiC + 12HNO_3 \rightarrow Ti(NO_3)_4 + CO_2 + 8NO_2 + 6H_2O \qquad (2)$$
$$Ti(NO_3)_4 + H_2O \rightarrow TiO(NO_3)_2 + 2HNO_3 \qquad (3)$$
$$TiO(NO_3)_2 + (x+1)H_2O \rightarrow TiO_2 \cdot xH_2O + 2HNO_3 \qquad (4)$$
$$4TiO(NO_3)_2 + TiC \rightarrow 5TiO_2 + 8NO_2 + CO_2 \qquad (5)$$
$$TiC + 8HNO_3 \rightarrow TiO_2 + 8NO_2 + CO_2 + 4H_2O \qquad (6)$$

It should be noted that the mole ratio of the reagents according to equation (6) is 1:8, which is higher than used during the synthesis (1:3). Thus, carbon in titanium carbide is oxidized not completely to CO_2, but also to CO, and partly oxidized carbon species can be preserved in the TiO_2 powder synthesized. The presence of such species in the as-prepared material is supported by the fact that after annealing the powder in an inert atmosphere (Ar) at 400 °C, its color is changed from yellowish to black. During the synthesis, nitric acid is reduced not only to NO_2, but also to N_2O_3, NO, N_2O and N_2. We observed the formation of a great amount of brown NO_2 gas, and some amount of N_2O_3 was detected. N_2O_3 caused appearance of blue coloration of water in a condenser.

The XRD data show that the TiC phase is completely oxidized in the end of the synthesis (Fig. 1). The evolution of a great amount of gases during the oxidation process favours formation of the mesoporous structure of TiO_2 powder, which is characterized by a large surface area (Fig. 2, Table 1). FTIR spectra demonstrate that TiO_2 powders annealed at 70 and 200 °C have a great amount of nitrate and nitro groups, which are differently coordinated on the oxide surface. According to the TG data, the most intensive elimination of nitrate-nitro groups is observed between 220 and 280 °C, and the FTIR spectrum of the TiO_2 sample annealed at 400 °C already indicates the absence of nitrate and nitro groups. The presence of these groups on the TiO_2 surface determines a high adsorptive capacity of the powder annealed up to 200 °C to positively charged dye (RhB). The sample annealed at 400 °C almost does not adsorb RhB in neutral solutions.

Surface nitrate and nitro groups may inhibit the growth of TiO_2 crystallites during heat treatment. The increase of the TiO_2 crystallite size and decrease of the powder surface area are observed at temperatures higher than the temperature of nitrate-nitro group decomposition. After annealing at 400 °C the titania particle size grows twice and

the surface area is reduced by about 2.5 times. Better crystallinity and less deficiency (these factors reduce the recombination of photogenerated electron-hole pairs in the oxide) of the samples annealed at 400 °C result in their higher photoactivity, as inferred from the RhB decomposition under UV irradiation, as compared with the sample annealed at 200 °C.

4. Conclusion

Mesoporous TiO_2 powders with large surface area and high porosity were synthesized from TiC by oxidation with HNO_3 at enhanced temperature. The multistep mechanism for titanium carbide oxidation is proposed.

Great amount of nitrate and nitro groups on the surface of as-synthesized TiO_2 powder is observed by FTIR spectroscopy. These surface nitrate-nitro groups determine adsorption properties of TiO_2 and influence morphological characteristics of the samples annealed at different temperatures. The TiO_2 powder annealed at 200 °C is characterized by a crystallite size of 3.9 nm, a surface area of 353 $m^2 g^{-1}$ and an adsorption capacity towards RhB of 35 mg g^{-1}. Annealing of TiO_2 powder at temperatures higher than the temperature of nitrate-nitro groups elimination leads to growth of TiO_2 crystallites, decrease in the porosity and surface area and lowering the adsorption capacity to the positively-charged dye. At the same time, improving the photocatalytic activity of the TiO_2 powder under UV irradiation is observed. The photoactivity of the sample annealed at 400 °C is close to commercial TiO_2 photocatalyst Degussa P-25 in the UV range.

Acknowledgements

We gratefully acknowledge the financial support of the European Commission (Project: 645662 – SMARCOAT - H2020-MSCA-RISE-2014) for this research.

References

[1] A.L. Linsebigler, G. Lu, J.T. Yates, Chem. Rev. 95 (1995) 735−758.
[2] K. Nakata, A. Fujishima, J. Photochem. Photobiol. C 13 (2012) 169–189.
[3] J. Schneider, M. Matsuoka, M. Takeuchi, J. Zhang, Y. Horiuchi, M. Anpo, D. W. Bahnemann, Chem. Rev. 114 (2014) 9919–9986.
[4] B. O'Regan, M. Gratsel, Nature 353 (1991) 737–740.
[5] W. Zhou, H. Fu, ChemCatChem 5 (2013) 885–894.
[6] Z. Bian, J. Zhu, J. Wang, S. Xiao, C. Nuckolls, H. Li, J. Am. Chem. Soc. 134 (2012) 2325–2331.
[7] A. Fujishima, T.N. Rao, D.A. Tryk, J. Photochem. Photobiol. C 1 (2000) 1–21.
[8] M.A Fox, M. Dulay, Chem Rev 93 (1993) 341–57.
[9] J.M. Herrmann, Catal. Today 53 (1999) 115–29.
[10] M. Ni, M. K. H. Leung, D.Y.C. Leung, K. Sumathy, Renew. Sust. Energ. Rev. 11 (2007) 401–425.
[11] P. Yang, D. Zhao, D.I. Margolese, B.F. Chmelka, G.D. Stucky, Nature 396 (1998) 152 –155.
[12] L. Robben, A.A. Ismail, S.J. Lohmeier, A. Feldhoff, D.W. Bahnemann, J. Buhl, Chem. Mater. 24 (2012) 1268–1275.
[13] D.M. Antonelli, J.Y. Ying, Angew.Chem. Int. Ed. Engl. 34 (1995) 2014–2017.
[14] J. Yu, L. Zhang, B. Cheng, Y. Su, J. Phys. Chem. C 111 (2007) 10582–10589.
[15] H. Wang, J. Miao, J. Zhu, H. Ma, J. Zhu, H. Chen, Langmuir 20 (2004) 11738–11747.
[16] X. Liu, Y. Gao, C. Cao, H. Luo, W. Wang, Langmuir 26 (2010) 7671–7674.
[17] J.B. Joo, Q. Zhang, I. Lee, M. Dahl, F. Zaera, Y. Yin, Adv. Funct. Mater. 22 (2012) 166–174.
[18] R.O. Da Silva, R.H. Galves, D.G. Stroppa, A.J. Ramirez, E.R. Leite, Nanoscale 3 (2011) 1910–1916.
[19] R. Bleta, P. Alphonse, L. Lorenzato, J. Phys. Chem. C 114 (2010) 2039–2048.
[20] S.H. Elder, Y. Gao, X. Li, J. Liu, D.E. McCready, C.F. Windisch, Chem. Mater. 10 (1998) 3140−3145.
[21] C. Liu, L. Fu, J. Economy, J. Mater. Chem. 14 (2004) 1187−1189.
[22] D. Huang, G.S. Luo, Y.J. Wang, Micropor. Mesopor. Mater. 84 (2005) 27−33.
[23] D.-L. Shieh, J.-S. Li, M.-J. Shieh, J.-L. Lin, Micropor. Mesopor. Mater. 98 (2007) 339–343.
[24] JCPDS: No 21-1272.
[25] K.S.W. Sing, D.H. Everett, R.A.W. Haul, L. Moscou, R.A. Piertti, J. Rouquerol, T. Siemieniewska, Pure & Appl. Chem. 57 (1985) 603–619.
[26] A.A. Davydov, Spectroscopy of Oxide Catalyst Surfaces, Wiley, Chichester, 2003.
[27] A.B. Lever, E. Mantovani, B.S. Ramaswamy, Can. J. Chem. 49 (1971) 1957–1964.
[28] U.I. Gaya, A.H. Abdullah, J. Photochem. Photobiol. C: Photochem. Rev. 9 (2008) 1–12.